



Fjrs.futa.edu.ng

# FUTA Journal of Research in Sciences

ISSN: 2315 – 8239 (Print); E-ISSN: 2489 - 0413



FUTA Journal of Research in Sciences, Vol. 14(1), April, 2018: 12-26

## A Green Approach to Corrosion Mitigation of Mild Steel in Acid Medium Using *Caesapinia Bonduc* Seed Coat Extract

Emmanuel, F. Olasehinde

Department of Chemistry, Federal University of Technology, Akure

### ABSTRACT

The inhibitory and adsorptive effects of ethanol extract of *Caesapinia bonduc* seed coat (EECBSC) on corrosion of mild steel in 1M H<sub>2</sub>SO<sub>4</sub> solution were investigated using gravimetric and electrochemical techniques. Experiments were performed by varying immersion period, concentration of the inhibitor and temperature. The results suggest that EECBSC acts as a good corrosion inhibitor for mild steel in acid medium. Inhibition efficiency increased with increasing concentration of the extract and temperature. Kinetics of the reaction with and without inhibitor follow a first order reaction and the half-lives of the metal increase as the concentration of the extract increases. The adsorption of the inhibitor on the mild steel surface in acid solution was found to obey the Langmuir adsorption isotherm. The activation and thermodynamic parameters of dissolution and adsorption processes were calculated and discussed. The mechanism of inhibition and formation of Fe-inhibitor complex was confirmed by FT-IR spectral analysis. Characterization of EECBSC was carried out using Fourier transform infrared spectroscopy and the results indicate that the inhibition of corrosion of mild steel occurs through adsorption of the inhibitor molecules. The scanning electron microscopy (SEM/EDX) result revealed the formation of a protective layer on the mild steel. Atomic Absorption Spectroscopy (AAS) analysis confirmed that the dissolution of iron (Fe<sup>2+</sup>) in the uninhibited solution was faster than the inhibited solution. Polarization measurements showed that the EECBSC extract acts as a mixed-type inhibitor.

**Keyword:** Gravimetric, Electrochemical; corrosion, Inhibition, *Caesapinia bonduc*; thermodynamics;

### INTRODUCTION

Corrosion is a naturally occurring phenomenon commonly defined as deterioration of metal surfaces caused by the reaction with the surrounding environmental conditions. It is typically an electrochemical process in which the corroding metal behaves like a small electrochemical cell. Electrochemical corrosion is the most common form of attack of metals, and it occurs when metal atoms lose electrons and become ions (Eddy, *et al.*, 2011). Common examples of metal corrosion are the rusting of iron, the tarnishing of silver, the dissolution of metals in acid solutions, and the growth of patina on copper (Fouda *et al.*, 2009). Scientists have

been trying to understand how to control corrosion for as long as iron and steel have been in use. Mild steel, the most widely used among them, is also highly susceptible to corrosion, especially in acidic media (Prabhu *et al.*, 2008). Generally, mild steel undergoes corrosion in processes such as acid pickling, industrial cleaning, acid descaling, oil well acidizing and petrochemical processes (Daniyan *et al.*, 2011; Okafor and Ebenso, 2007). Meanwhile, H<sub>2</sub>SO<sub>4</sub> is one of the most widely used acids in several industries for the removal of undesirable oxide films and corrosion products of the surface of steel, hence, the choice of this acid in this study.

Among various methods of reducing the corrosion rate of metals and alloys, the use of inhibitors is one of the most efficient alternatives especially in acidic media due to its advantages of economy, high efficiency and wide applicability. The principle of corrosion inhibition is to prevent the chloride ions from reacting with the steel surface. Thus, corrosion inhibitors are chemical substances which decrease corrosion rate when present in the corrosion system at a suitable concentration without significantly changing the concentration of any other corrosive agent (Daniyan *et al.*, 2011, Obot *et al.*, 2010). Corrosion inhibition of metals may involve either physiosorption or chemisorption of inhibitors onto the metal surface and subsequent interference with either cathodic, or anodic, or both reactions occurring at the adsorption sites (Zhang *et al.*, 2012; Awad, 2006). Different types of organic compounds have been widely reported to act as corrosion inhibitors. These compounds contain heteroatoms such as sulphur, phosphorus, nitrogen, or oxygen, and multiple bonds, which act through a process of surface adsorption. The adsorption occurs due to the interaction of the lone pair or  $\pi$ -orbitals of inhibitor molecules with d-orbitals of the metal surface atoms. However, in spite of their high inhibition efficiency and good protection for metals, their toxicity and carcinogenic properties are significant (Ebenso *et al.*, 2004). Hence, investigations are focused toward the development of naturally occurring substances as ecofriendly corrosion inhibitors. Due to bio-degradability, ecofriendliness, low cost and easy availability, the extracts of some common plants based chemicals and their by-products have been investigated as inhibitors for metals under different environments (Kliskic *et al.*, 2000; Ebenso *et al.*, 2004; Abdel-Gaber *et al.*, 2006).

*Caesalpinia bonduc*, commonly known as Gray Nicker nut is a prickly shrub with grey, hard, globular shaped seeds and a smooth shining surface. It is a medicinal plant predominantly distributed in the tropical and subtropical regions

of Africa, Asia and the Caribbean. Previous researchers have shown that the leaves, seeds and roots of the plant contain some hydroxyl organic compounds such as flavonoids, phenols, diterpenoids and steroids (Sivasankari *et al.*, 2010.), which makes it suitable to be a potential corrosion inhibitor. However, literature survey revealed that no study has been conducted on the inhibitive properties of EECBSC on mild steel in acidic medium. Therefore, we have investigated the inhibitory and adsorptive effects of EECBSC on mild steel in acidic medium using gravimetric and electrochemical methods.

## MATERIALS AND METHODS

### Mild steel

Mild steel specimen with the following composition (wt.%): 0.12% C, 0.17% Si, 0.56% Mn, 0.02% P, 0.03% S, 0.11% Ni, 0.08% Cr and bal. Fe were used for weight loss and electrochemical studies. The metal samples were prepared, degreased and cleaned as previously described (Olasehinde *et al.*, 2013, 2015). Weight of the metal samples was taken using Mettler AE 160 analytical balance. Analytical grade reagents were used for the study.

### Preparation of the extract

*Caesalpinia bonduc* plant was obtained from Aramoko-Ekiti in Ekiti State, Nigeria. The plant material was dried and seeds were broken so as to separate the kernel and the seed coat. The seed coat was pulverized and sieved through a mesh (850-micron meter sieve). Ethanol extract of the powdered sample was obtained by soaking 500 g of the sample in 2.5 L of ethanol for 4 days at room temperature, after which the mixture was filtered with whatman no.1 filter paper. The filtrate was further subjected to evaporation over a boiling water bath and finally, a deep-brown solid residue was obtained and preserved in a desiccator. The corrosion test solutions were prepared by dissolving specified amount of EECBSC in 1 M  $H_2SO_4$  solution and used for corrosion study.

### Weight loss measurement

The weight loss method employed in this study has been described elsewhere (Olasehinde *et al.*, 2013, 2015). The mild steel coupons of dimension 17 mm × 14 mm × 13 mm were used for the weight loss measurement. The coupons were weighed and completely immersed in 100 mL of 1M H<sub>2</sub>SO<sub>4</sub> with and without the additions of various concentrations of the inhibitor with the aid of glass hooks at different temperatures (303, 313, 323 and 333 K) for 4 hours. The kinetic data was obtained by immersing mild steel in the test solution for five days (24, 48, 72, 96 and 120 h) at room temperature. After the pre-set immersion time, mild steel was withdrawn from the test solution, washed with distilled water, rinsed in acetone, dried and re-weighed accurately. The experiments were carried out in triplicate, and the mean values were reported. The difference in the weight of the mild steel before and after immersion is taken as the weight loss. The corrosion rate (C<sub>R</sub>) of mild steel was determined using the relation:

$$C_R = \frac{\Delta w}{At} \quad (1)$$

where  $\Delta w$  is the weight loss in grammes, A is the cross-sectional area in cm<sup>2</sup> and t is the exposure time in hours. The inhibition efficiency (I.E) and surface coverage ( $\theta$ ) were determined using the following equations:

$$I. E. (\%) = 1 - \left( \frac{C_{R_2}}{C_{R_1}} \right) \times 100 \quad (2)$$

$$(\theta) = 1 - \left( \frac{C_{R_2}}{C_{R_1}} \right) \quad (3)$$

Where C<sub>R1</sub> and C<sub>R2</sub> are the corrosion rates of the mild steel strip coupons with and without inhibitor, respectively.

### Electrochemical measurement

The electrochemical experiments were carried out using AUTOLAB PGSTAT 204N instrument, piloted by Nova software. The experiments were performed using a three-electrode corrosion cell set-up consisting of mild steel as the working

electrode (surface area = 1cm<sup>2</sup>), saturated silver/silver chloride as reference electrode, and platinum rod as counter electrode. The test electrolyte was solution of H<sub>2</sub>SO<sub>4</sub> in the presence and absence of the extract. The working electrode was immersed in a test solution for 30 minutes until a stable open circuit potential was attained. The working electrodes were prepared by attaching an insulated copper wire to one face of the sample using an aluminum conducting tape, and cold mounting it in resin. Potentiodynamic polarization measurements were carried out using a scan rate of 1.0 mV/s at a potential initiated at -250mV to +250mV with respect to OCP. After each experiment, the electrolyte and the test sample were replaced. The linear Tafel segments of the anodic and cathodic curves were extrapolated to corrosion potential to obtain the corrosion current densities (I<sub>corr</sub>) and corrosion potential (E<sub>corr</sub>). Anodic Tafel slope ( $\beta_a$ ) and cathodic Tafel slopes ( $\beta_c$ ) were determined from the experimental curve. The I<sub>E<sub>corr</sub></sub>(%) was calculated using the current densities.

$$I_{E_{corr}} (\%) = \frac{I_{corr}^0 - I_{cor}}{I_{corr}^0} \times 100 \quad (4)$$

### Surface Morphology Examination

The chemical composition of the corrosion product and the formation of a passive layer on the surface of the mild steel in the absence and presence of inhibitor were examined using Scanning Electron Microscope (SEM). The surfaces of the mild steel were viewed under SEM (Nikon Eclipse ME 6000) coupled with EDX detector. The mild steel specimens were immersed in 1 M H<sub>2</sub>SO<sub>4</sub> solution in the absence and presence of EECBSC for 4 h after which, they were removed, washed with distilled water and allowed to dry at room temperature. The chemical composition of the corrosion products was recorded with an EDX detector coupled with the SEM.

### FT-IR characterization of plant

The EECBSC was characterized by Fourier transform infrared (FT-IR) spectroscopy. Finely

powered Mild Steel specimen was immersed separately in solution of H<sub>2</sub>SO<sub>4</sub> containing the extract for 4 hours to form the adsorption product. FT –IR spectrum was recorded for the extract and the adsorption product. These spectra were recorded in a Perkin-Elmer-1600 spectrophotometer using KBr pellets with the frequency ranging from 4000 to 400 cm<sup>-1</sup>.

#### Atomic Absorption Spectroscopy (AAS) Analysis

The dissolution of Iron (II) ions in both inhibited and uninhibited solutions was monitored using Atomic Absorption Spectrometer model Buck Scientific 210. The coupons were immersed in 100 mL of 1 M H<sub>2</sub>SO<sub>4</sub> with and without various weights of the inhibitor. After 4 hours of immersion, the coupons were removed and the solutions were filtered and the filtrates were used for the analysis. This was done in order to determine the amount of iron (II) ions dissolved in both inhibited and uninhibited solution after 4 hours of immersion. The calibration curve of iron (II) ions was drawn before analyzing the electrolyte solution. All samples containing iron (II) were diluted with distilled water to ensure that the concentration of the metal ions is within the

range of the calibration curve (Alaneme *et al.*, 2016).

## RESULTS AND DISCUSSIONS

### Weight loss study

The corrosion rate and inhibition efficiency of mild steel specimens as a function of the extract concentration in 1 M H<sub>2</sub>SO<sub>4</sub> solution monitored at room temperature is summarized in Table 1. The result obtained showed that the rate of corrosion of mild steel in 1 M H<sub>2</sub>SO<sub>4</sub> decreases in response to the additions of increasing amounts of EECBSC to the corrosive medium. Specifically, the corrosion rate of the mild steel coupons after the addition of EECBSC markedly decreases as the concentration of the extract increases up to 0.4g/100 mL and beyond this concentration, the decrease becomes less noticeable while the inhibition efficiency increases monotonically with increase in the concentration EECBSC. This suggests that as the concentration of the extract increases, there is an increase in the number of adsorption of the extract constituents on the surface of the mild steel which provides a barrier for mass transfer and prevents further corrosion (Ebenso *et al.*, 2004; Olasehinde *et al.*, 2015., ; Patricia *et al.*, 2018).

**Table 1:** Corrosion rate and inhibition efficiency of different concentration of EECBSC on mild steel at room temperature.

Inhibitor Concentration (g/ 100 mL)	Corrosion Rate gcm <sup>-2</sup> h <sup>-1</sup>	Inhibition Efficiency (%)
0.2	0.00233	60.22
0.4	0.00098	68.68
0.6	0.00074	70.62
0.8	0.00063	72.55
1.0	0.00054	77.99

### Effect of temperature and thermodynamics

Experimental results obtained from weight loss measurements for mild steel with and without different concentrations of EECBSC at various temperatures are presented in Fig. 1. Inspection of the plot shows that as the reaction temperature increases from 303-343 K, the inhibition efficiency increases. Previous investigators have

reported that increase in inhibition efficiency as a result of increase in temperature suggests that the adsorption of the inhibitor on mild steel surface is consistent with the mechanism of chemical adsorption. For a physical adsorption mechanism, inhibition efficiency of an inhibitor is expected to decrease with temperature while a for chemical adsorption mechanism, values of inhibition

efficiency increase with temperature (Patricia *et al.*, 2018; Ating *et al.*, 2010; Ebenso *et al.*, 2004). In this study, the inhibition efficiency of EECBSC increases with temperature suggesting that the

adsorption of the EECBSC on mild steel surface is consistent with the mechanism of chemical adsorption

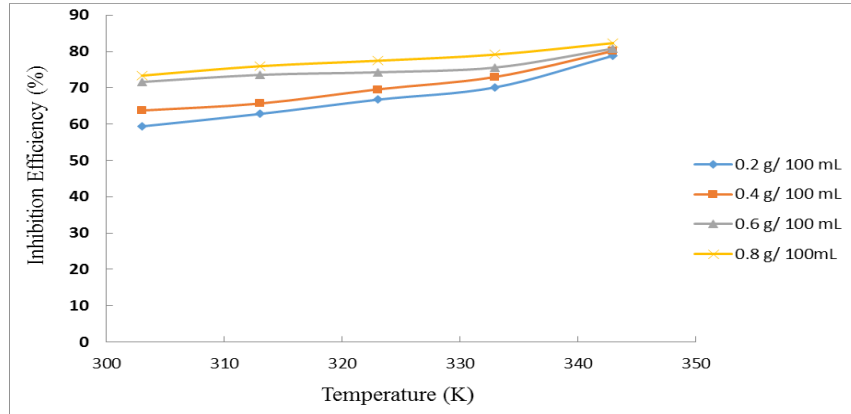


**Figure 1.** A plot of inhibition efficiency against temperature at different concentrations of EECBSC

The activation energy ( $E_a$ ) for mild steel corrosion reaction at different inhibitor concentrations was calculated from the slope of the Arrhenius plot ( $\log C_R$  vs.  $1/T$ ) (Fig. 2), where the slope is  $E_a/2.303 R$ ,  $C_R$  is corrosion rate,  $R$  is molar gas constant and  $T$  is the temperature in absolute scale. These values are given in Table 2 and it is evident from the Table that the calculated values of  $E_a$  for

the inhibited system are found to be lower than the uninhibited system. It has been established in the literature that decrease in activation energy in the presence of the inhibited system compared to uninhibited system may be interpreted as chemical adsorption (Ebenso *et al.*, 2004; Awad, 2006; Olasehinde *et al.*, 2015). Thus, the mode of inhibition of EECBSC on mild steel in  $H_2SO_4$  is suggestive of chemical adsorption mechanism.

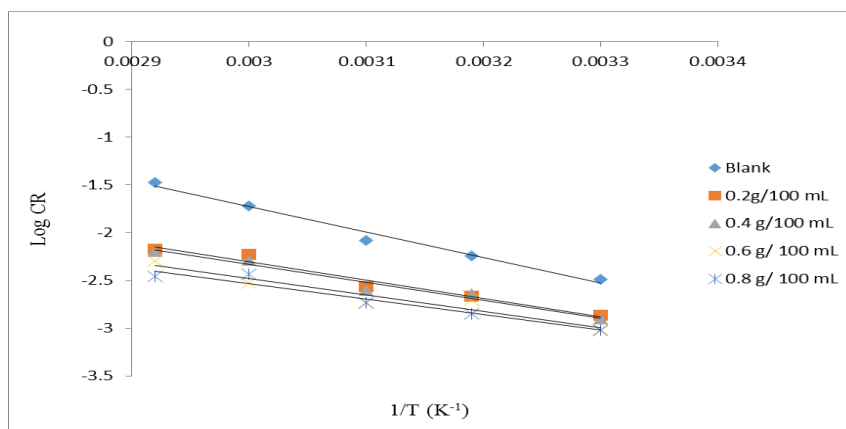


**Figure 2.** Arrhenius plot for mild steel in 1 M  $H_2SO_4$  in the absence and presence of EECBSC.

The change in enthalpy ( $\Delta H^*$ ) and entropy ( $\Delta S^*$ ) of activation were calculated by the Eyring transition-state equation given Transition State equation ( eqn 5 )

$$CR = \left[ \frac{RT}{Nh} \right] \exp \left[ \frac{\Delta S^\ddagger}{R} \right] \exp \left[ \frac{-\Delta H^\ddagger}{RT} \right] \quad (5)$$

Where  $h$  is the plank's constant,  $N$  is the Avogadro's number,  $T$  is the absolute temperature,

$R$  is the universal gas constant,  $\Delta S^\ddagger$  is the entropy of activation and  $\Delta H^\ddagger$  is the enthalpy of activation. Fig. 3 shows a plot of  $\text{Log} ( CR/T )$  as a function of  $1/T$ . Straight lines were obtained with a slope of  $( -\Delta H^\ddagger / 2.303R )$  and an intercept of  $\text{Log} R/Nh + \Delta S^\ddagger / 2.303 R$ , from which the values of  $\Delta S^\ddagger$  and  $\Delta H^\ddagger$  were calculated as presented in Table 2.

**Table 2.** Calculated values of thermodynamic parameters for the corrosion of mild steel in 1M H<sub>2</sub>SO<sub>4</sub> with EECBSC

Concentration (g/100 mL)	$\Delta S$ (kJ/mol/K)	$\Delta H$ (kJ /mol)	Ea (kJ/mol)
Blank	-0.0801	47.16	51.24
0.2	-0.1107	40.29	36.69
0.4	-0.1185	37.97	35.79
0.6	-0.1274	35.75	32.89
0.8	-0.1364	33.07	31.23

Inspection of data presented in Table 2 shows that the positive values of  $\Delta H^\ddagger$  both in the absence and presence of the extract reflect the endothermic nature of the mild steel dissolution process. It is also evident that the activation enthalpies vary in the same manner as activation energies, supporting the inhibition mechanism (Fouda *et al.*, 2009). The negative values of entropy ( $\Delta S^\ddagger$ ) implies that the activated complex in the rate determining step

represent association rather than dissociation, implying that disorderliness reduces on going from reactant to activated complex. The well oriented inhibitor would have reduced the dissolution of mild steel in H<sub>2</sub>SO<sub>4</sub> solution and thereby inhibiting it from the aggressive media. Similar observation has been reported in the literature (Fouda *et al.*, 2009; Ebenso *et al*, 2004; Olasehinde *et al.*, 2015)

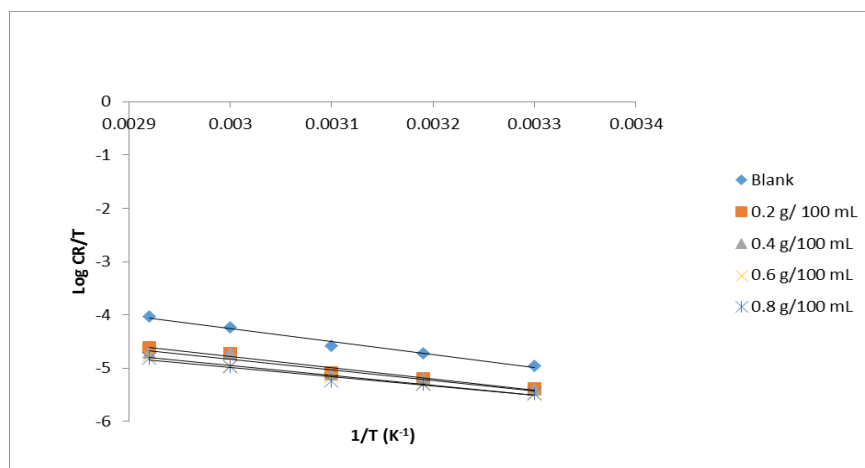


**Figure 3.** Eyring transition state plot for mild steel in 1M H<sub>2</sub>SO<sub>4</sub> in the absence and presence of EECBSC.

**Effect of Immersion Time**

Effect of time on the corrosion rate of mild steel in 1M H<sub>2</sub>SO<sub>4</sub> was investigated with and without different concentrations of EECBSC. The plot of ln (W<sub>1</sub>- ΔW) against time for the adsorption of EECBSC on mild steel is shown in Figure 4. The plot is linear which shows that the data points are well fitted into first order kinetics. The rate constant of the reaction process at different concentrations of the inhibitor was obtained from

the slope of the graph, and the half-lives were calculated from the rate constant using equation 6.

$$t_{1/2} = \frac{0.693}{k} \tag{6}$$

The calculated values of k and half-lives are listed in Table 3. The results showed that the half-lives of the metal increase as the concentration of the extract increases suggesting that inhibition efficiency increases with increase in the concentration of the extract.

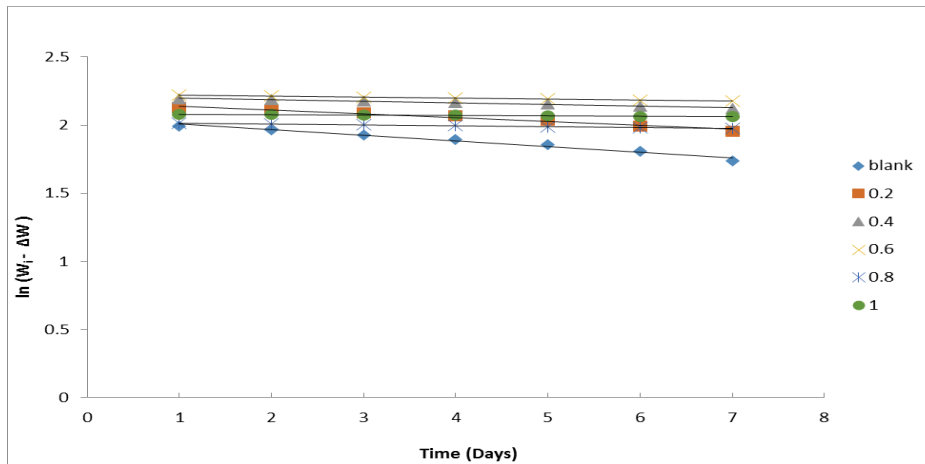


**Figure 4: First order plot of ln (W<sub>1</sub>- ΔW) against Time for the adsorption of EECBSC on mild steel at room temperature**

**Table 3: Kinetic data for mild steel corrosion in 1 M H<sub>2</sub>SO<sub>4</sub> in the absence and presence EECBSC**

Concentration (g/100 mL)	Rate constant (day <sup>-1</sup> )	Half-lives (days)
Blank	0.0944	7.33
0.2	0.0645	10.74
0.4	0.0276	25.07
0.6	0.0161	42.98
0.8	0.0138	50.15
1.0	0.0069	100.30

**Adsorption isotherm**

The adsorption isotherms are used to investigate the mode of adsorption and the characteristics of adsorption of inhibitor on the metal surface (Eddy *et al.*, 2011). The interaction between the inhibitors and the steel surface can be described by

the adsorption isotherm. The most frequently used adsorption isotherms are Frumkin, Temkin, Freundlich, Florry Huggins, Bockris-Swinkel, El-Awardy and Langmuir isotherms. All of these isotherms are of the general form;

$$f(\Theta, x) \exp(-2a\Theta) = kC \quad (7)$$

where  $f(\Theta, x)$  is the configurational factor which depends upon the physical model and assumption underlying the derivative of the isotherm,  $\Theta$  is the surface coverage,  $C$  is the inhibitor concentration,  $x$  is the size ratio, “ $a$ ” is the molecular interaction parameter, and  $K$  is the equilibrium constant of adsorption process (Alaneme, *et al.*, 2016). The surface coverage ( $\Theta$ ) values help in understanding adsorption characteristics. The degree of surface coverage values for different concentrations of EECBSC obtained at different temperatures from weight loss measurement were calculated using equation below:

$$\text{Surface coverage } (\Theta) = \frac{\% \text{ I.E}}{100} \quad (8)$$

Adsorption behaviour of EECBSC can be explained by Temkin, Langmuir and Freundlich adsorption isotherms. Therefore, attempts were made to fit to the various isotherms and it was found that the best fit was obtained with Langmuir isotherm. Langmuir isotherm is an ideal isotherm for physical or chemical adsorption where there is no interaction between the adsorbate and adsorbent. It can be expressed according to equation 9:

$$\frac{c}{\Theta} = \frac{1}{k_{ads}} + C \quad (9)$$

Where  $C$  is the concentration of the inhibitor,  $K_{ads}$  is the adsorption equilibrium constant and  $\Theta$  is the degree of surface coverage of the inhibitor. A plot of  $C/\Theta$  against  $C$  is expected to be linear. As shown in Figure 5, the high correlation coefficient

( $R^2$ ) of the adsorption isotherm data suggested that the adsorption of this inhibitor can be fitted to the Langmuir adsorption isotherm. This implies that the adsorbing EECBSC occupy typical adsorption site at the metal/solution surface. The slope of unity obtained in this study is an indication that the adsorption of the components is approximated by Langmuir adsorption isotherm and that the monolayer of the inhibitor species on the mild steel surface without lateral interaction between adsorbed species is postulated. From the intercept in Fig. 5, values of  $k_{ads}$  were calculated. The large value of  $k_{ads}$  obtained for the inhibitor imply efficient adsorption and good corrosion inhibition efficiency. Using the calculated values of  $k_{ads}$ ,  $\Delta G_{ads}$  was evaluated according to the equation 10.

$$K_{ads} = \frac{1}{55.5} \exp\left(\frac{-\Delta G_{ads}}{RT}\right) \quad (10)$$

This equation can also be expressed as follows:

$$\Delta G_{ads} = -2.303RT \text{ Log } (55.5K_{ads}) \quad (11)$$

$K_{ads}$  is the equilibrium constant of adsorption process,  $R$  is the universal gas constant with the value of  $8.314 \text{ J mol}^{-1}\text{K}^{-1}$ ,  $T$  is the temperature and  $\Delta G_{ads}$  is the Gibbs free energy of adsorption and 55.5 is the molar concentration of water in solution.



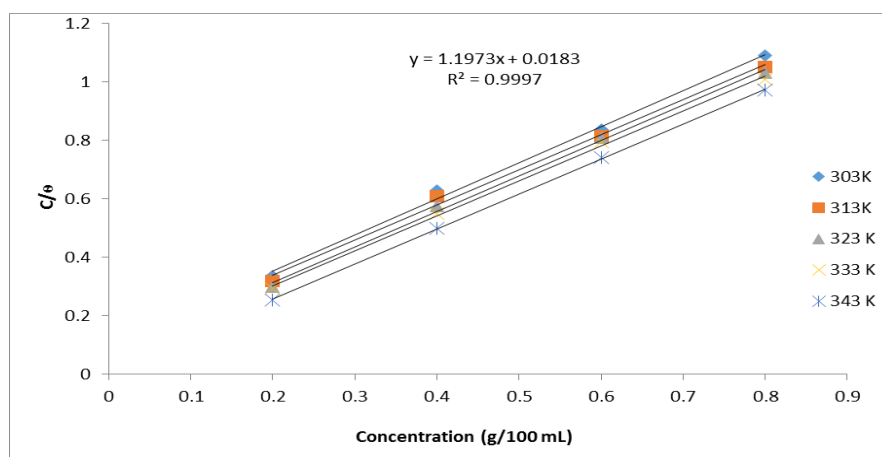


**Figure 5. Langmuir adsorption isotherm plot for mild steel corrosion in 1 M H<sub>2</sub>SO<sub>4</sub> for EECBSC at different temperatures**

The values of  $\Delta G_{\text{ads}}$  were negative in all the temperature as shown in Table 4. This indicates the spontaneous adsorption of extracts on surface of mild steel in H<sub>2</sub>SO<sub>4</sub> acid solution. It is well known that values of  $\Delta G_{\text{ads}}$  less negative than -20 kJ/mol are associated with the physical adsorption involving electrostatic interaction between charged molecules and a charged metal while those around -40 kJ/mol or higher are associated with charge sharing or transfer from the inhibitor molecules to the metal surface to form a coordinate type of bond (which indicates chemisorption). Accordingly, the values of  $\Delta G_{\text{ads}}$  obtained in the present study are below -20 kJ/mol except for the reaction carried out at 343 K which was -22.92 kJ/mol. Thus, the mode of adsorption could be described as physical and chemical adsorption mechanisms. (Lebrini *et al.*, 2010, Umoren *et al.*, 2014; Khadom *et al.*, 2018).

It should be noted that the results of the present study revealed that EECBSC inhibits the acid induced corrosion of mild steel by virtue of adsorption of its components onto the metal surface. The inhibition process is a function of the metal, inhibitor concentration, and temperature as well as inhibitor adsorption abilities which is so much dependent on the number of adsorption sites. The mode of adsorption (physio-sorption and chemisorption) observed could be attributed to the fact that *Caesaphinia bonduc* seed coat extract contains many different chemical compounds some of which can be adsorbed chemically and others physically on the surface of the mild steel. Similar observations have been reported by previous investigators (Moorthy *et al.*, 2012; Ating *et al.*, 2010).

**Table 4. Calculated parameters from Langmuir adsorption Isotherm plot for EECBSC**

Temperature (K)	Slope	R <sup>2</sup> values	(K <sub>ads</sub> ) L/g	(ΔG) (kJ/mol)
303	1.234	0.996	9.52	-15.79
313	1.203	0.995	10.30	-16.52
323	1.214	0.997	14.08	-17.89
333	1.198	0.998	16.12	-18.81
343	1.197	0.999	55.55	-22.92

### Surface Morphology Examination

The surface morphologies of the mild steel samples in 1M H<sub>2</sub>SO<sub>4</sub> solution in the absence and

presence of EECBSC were shown in Figs. 6. The surface analysis using scanning electron microscope provides more information on the

level of attack as well as inhibition ability of the extracts on the surface of the mild steel. Analysis of the micrograph before immersion shows a fine and smooth surface indicating a good state of the mild steel as shown in Fig 6a. The rough surface obtained (Fig 6b) when the metal was immersed in 1M H<sub>2</sub>SO<sub>4</sub> solution for 4 hours without inhibitor indicates significant corrosion. However, in Fig 6c, with the addition of inhibitor, the surface improved markedly in terms of smoothness,

indicating a considerable reduction of the corrosion rate. This implies that the extracts formed protective film over the surface of the mild steel thereby decreasing the mild dissolution in acidic medium. The inhibitor prevents direct and intensive attack on the metal. The surface morphology of the adsorbed protective film on the mild steel surface confirmed the high performance of inhibitive effect of the EECBSC.

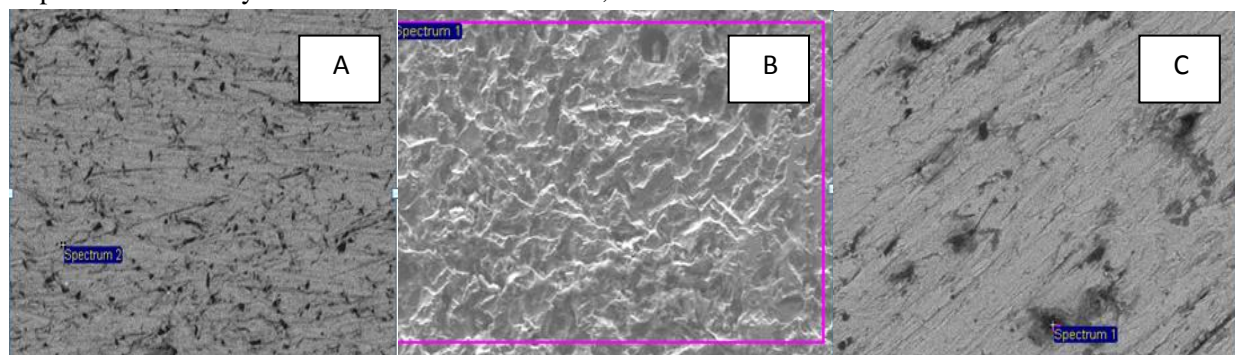


**Figure 6.** (A) SEM micrographs of mild steel sample prior to corrosion study; (B) SEM micrographs of mild steel samples after immersion in 1.0 M H<sub>2</sub>SO<sub>4</sub> solution without inhibitor; and (C) SEM micrographs of mild steel samples after immersion in 1 M H<sub>2</sub>SO<sub>4</sub> solution for 4hours in the presence of 1g/100 mL EECBSC.

#### FT-IR characterization of EECBSC

The inhibition performance of plant extract is normally ascribed to the presence in their composition of organic compounds containing polar functions with N, S, O atoms as well as conjugated double bond or aromatic rings. Fig. 7 and Fig. 8 show the IR spectra of ethanolic extracts of *Caesaphilia bonduc* seed coat and the corrosion product on the surface of mild steel in the presence of the inhibitors. The absorption band between 3300 cm<sup>-1</sup> to 3500 cm<sup>-1</sup> is attributed to N-H/O-H bond stretching vibration (Li *et al.*, 2010; Abder-Gaber *et al.*, 2006; Hefang *et al.*, 2016). Extract of *Caesaphilia bonduc* seed coat shifted from 3407 cm<sup>-1</sup> to 3396 cm<sup>-1</sup> when adsorbed on the surface of the mild steel. This shifting in the frequencies may imply that the active phytochemical constituents present in the inhibitor molecules bind to the metal surface to form a

protective metal inhibitor complex to reduce further dissolution of metal in the aggressive media. There was another shift from 2357 cm<sup>-1</sup> to 2356 cm<sup>-1</sup> and another backward shift from 1647 cm<sup>-1</sup> to 1646 cm<sup>-1</sup>. These bands imply the presence of C-H and C=O groups, respectively (Hefang *et al.*, 2016; Khadom *et al.*, 2018). The absorption bands between 1117 cm<sup>-1</sup> to 1140 cm<sup>-1</sup> observed in the samples correspond to C-O-C stretching vibration and bands below 1000 cm<sup>-1</sup> are attributed to the presence of C-C, C-O and C-N (Khadom *et al.*, 2018). The changes in absorption bands suggest that the adsorption between extract and mild steel took place through these functional groups. The results indicate that *Caesaphilia bonduc* seed coat extract contains O, and N atoms in functional groups (O-H, N-H, C-O, C=O, C-H) and aromatic rings which meet the general consideration of a typical corrosion inhibitor.

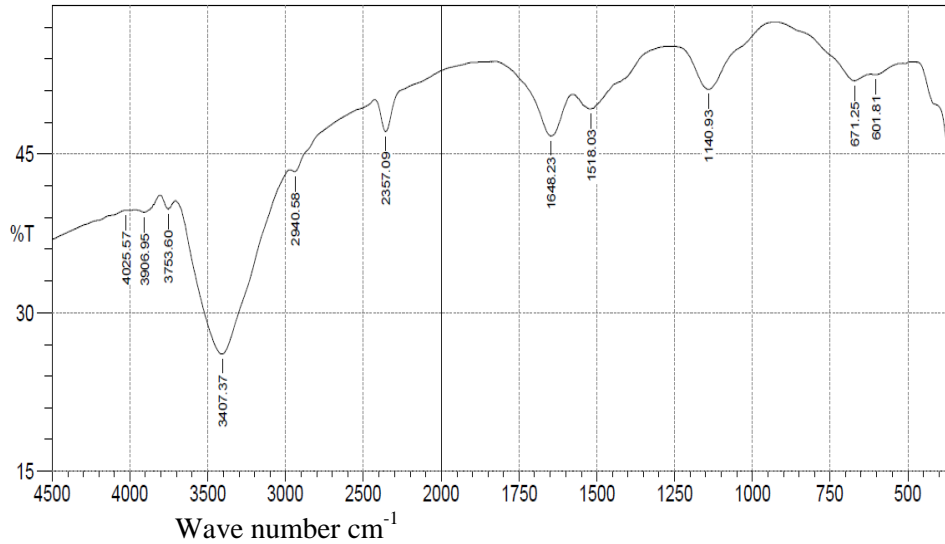


**Figure 7. FT-IR spectrum of EECBSC**

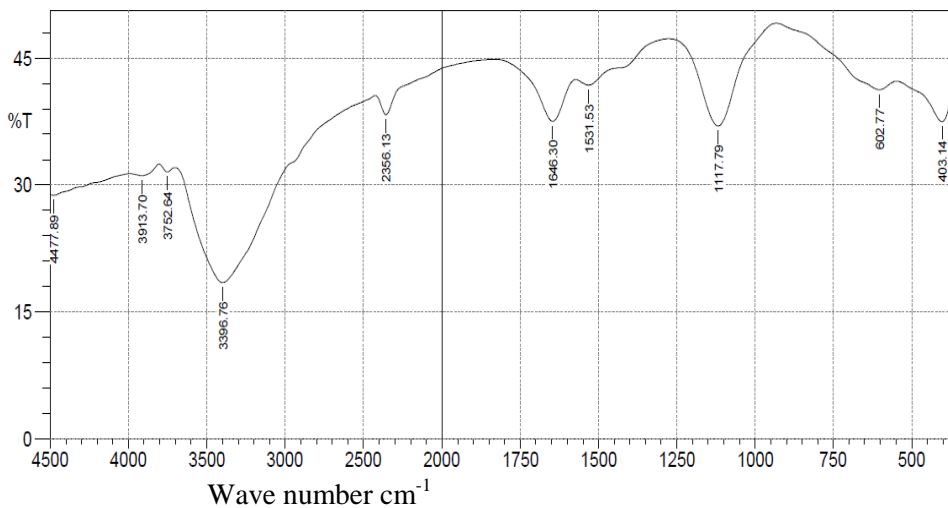


**Figure 8. FT-IR spectrum of dried solid absorption product of EECBSC on mild steel**

**Atomic Absorption Spectroscopy Analysis**

The plot of the dissolution of iron (II) ion against various concentration of EECBSC is shown in Figure 9. It was observed that there was steady reduction in the concentrations of Fe<sup>2+</sup> in solution as the concentration of the extract increased. This reduction in the concentration of Fe<sup>2+</sup> is due to the adsorption of the extract on the surface of the iron filling in the acidic media which resulted in the

resistance of the iron ion against rapid oxidation of Fe to Fe<sup>2+</sup>. Hence, the reduction observed in the Fe<sup>2+</sup> concentration in inhibited solution shows that the extract has been able to retard the corrosion rate of the iron in the acid solution. The percentage of Fe<sup>2+</sup> in the blank is the highest while the percentage of Fe<sup>2+</sup> decreases as the concentration of inhibitor increases. Similar results have been reported earlier (Fadare *et al.*, 2016).

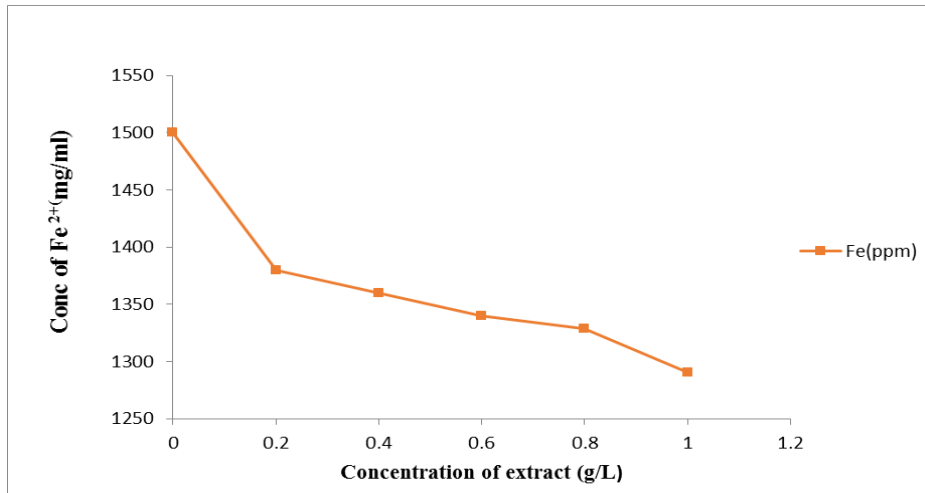


**Figure. 9. A plot of iron (II) ion dissolved in 1 M H<sub>2</sub>SO<sub>4</sub> against various concentrations of EECBSC**

**Potentiodynamic polarization**

The potentiodynamic polarizations curve for the mild steel in 1M H<sub>2</sub>SO<sub>4</sub> in the absence and presence of various concentrations of *Caesaphinia bonduc* seed coat extracts were shown in Fig. 10. The electrochemical parameters such as corrosion rate, the cathodic Tafel slope ( $\beta_c$ ), the anodic Tafel slope ( $\beta_a$ ), the current densities ( $I_{corr}$ ) and the corrosion potential ( $E_{corr}$ ) values obtained from the polarization curves for the extract are listed in Table 5. Inspection of the polarization curves and

electrochemical parameters reveals that the  $I_{corr}$  decrease considerably in the presence of the extract in acidic medium. It is also evident in (Fig. 10) that the presence of EECBSC affects both the cathodic and anodic parts of the curves indicating that the extracts influence the dissolution of the metal and the hydrogen evolution process. This is evident in the change in the anodic and cathodic slope values of inhibited with respect to uninhibited solution.

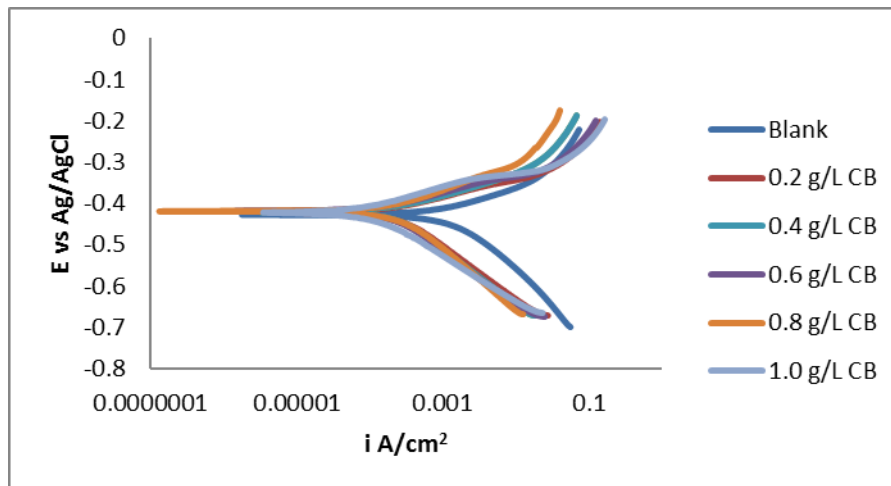


**Figure 10. Potentiodynamic polarization curves for mild steel in 1M H<sub>2</sub>SO<sub>4</sub> without and with various concentration**

It should be noted that the change in corrosion potential was from 6 to 22 mV in the presence of EECBSC compared to the blank. An inhibitor can be classified as a mixed type inhibitor if the displacement in corrosion potential is less than 85mV with respect to corrosion potential of the blank (Fadare, *et al.*, 2016; Zhang *et al.*; 2012; Umorent *et al.*, 2014; Moorthy *et al.*, 2012 ). Since the displacement of the corrosion potential is not up to 85mV (Table 5) after the addition of the extracts, it suggests that the inhibitor acts as a mixed-type inhibitor with predominant cathodic effectiveness. Corrosion inhibition efficiencies for the polarization reactions were estimated using Eqn.(12) and the values are listed in Table 5.

$$\eta_p \% = \frac{I_{corr} - I_{corr}(inh)}{I_{corr}} \times 100 \quad (12)$$

where  $I_{corr}$  represents the corrosion current density of the mild steel in 1M  $H_2SO_4$  in the presence of different concentration *Caesaphinia bonduc* seed coat extracts. From the Table , it is observed that the  $I_{corr}$  values gradually decreased with concomitant in the concentration of the extract. Thus, the inhibition efficiency increases with increase in the concentration of *Caesaphinia bonduc* seed coat extracts reaching the values of 90.4% at the optimum concentration (1.0 g/L) studied.

**Table 5. Potentiodynamic polarization for parameters mild steel in 1 M  $H_2SO_4$  in absence and presence of EECBSC.**

Extract conc.(% v/v)	$E_{corr}$ (mV)	$I_{corr}$ ( $\mu A/cm^2$ )	$\beta_a$ (mV/dec)	$\beta_c$ (mV/dec)	Corrosion rate(mm/year)	Inhibition efficiency (%)
blank	-428.7	1038	66.676	120.237	12.06	
0.2	-422.1	273.3	62.425	151.683	3.17	73
0.4	-420.5	231.6	55.821	141.181	2.50	77.7
0.6	-414.3	177.5	55.413	123.235	1.91	82.9
0.8	-411.2	168.2	58.276	126.327	2.90	83.8
1.0	-402.9	88.2	53.764	99.875	1.02	90.4

**CONCLUSIONS**

The extracts from *Caesaphinia bonduc* seed coat were found to be effective green inhibitors of mild steel corrosion in 1 M  $H_2SO_4$ . Inhibition efficiency of the extract increases with increase in concentration of the inhibitor and also with increase in temperature. The adsorption of different concentration of the extract on the surface of the mild steel in 1M  $H_2SO_4$  conforms to Langmuir adsorption isotherm. The FT-IR spectra indicate EECBSC contains O, and N atoms in functional groups (O-H, N-H, C-O, C=O, C-H) and aromatic rings which meet the general consideration of a typical corrosion inhibitor. The activation and thermodynamic parameters indicate that the adsorption process EECBSC onto the mild steel surface was by physisorption and

chemisorption. Kinetics of the reaction follows a first order reaction and the half-lives of the metal increase as the concentration of the extract increases. Surface analysis shows that there were some improvements on the surface morphology after the addition of inhibitor. The polarization studies showed that EECBSC acts as a mixed-type inhibitor.

**REFERENCES**

**Abdel-Gaber, A.M., Abd-El-Nabey, B.A., Sidahmed, I.M., El-Zayady, A.M., Saadawy, M.** (2006) Inhibitive action of some plant extracts on the corrosion of steel in acidic media, *Corros. Sci.* 48(9), 2765-2779

- Ating, E. I., Umoren, S. A., Udousoro, I. I., Ebenso, E. E., Udoh, A. P.,** (2010). Leaves extract of *ananas sativum* as green corrosion inhibitor for aluminium in hydrochloric acid solutions. *Green Chemistry Letters and Reviews*, 3( 2), 61–68.
- Awad MI** (2006). Eco friendly corrosion inhibitors: Inhibitive action of quinine for corrosion of low carbon steel in 1 m HCl. *J. Appl. Electrochem.* 36, 1163-1168.
- Alaneme, K. K . Olusegun, S.J. Alo, A.W.** (2016). Corrosion inhibitory properties of elephant grass (*Pennisetum purpureum*) extract: Effect on mild steel corrosion in 1 M HCl solution. *Alex. Eng. Journal* 55 (2), 1069-1076.
- Daniyan, A.A., Ogundare, O., Attah-Daniel, B.E., Babatope, B.** (2011). Effect of palm oil as corrosion inhibitor on ductile iron and mild steel. *Pac. J. Sci. and Tech.*, 12(2): 45-53.
- Ebenso, E. E., Ibok, U. J., Ekpe, U. J., Umoren, S., Jackson, E., Abiola, O. K., Oforka, N. C. , Martinez S.** (2004) Corrosion inhibition studies of some plant extracts on aluminium in acidic medium. *Transactions of SAEST.* 39(4): 117-123.
- Eddy, N.O., Awel, F.E., Gimba1, C.E., Ibis, N.O., Ebenso, E.E.** (2011). QSAR, experimental and computational chemistry simulation studies on the inhibition potentials of some amino acids for the corrosion of mild steel in 0.1 M HCl. *Int. J. Electrochem. Sci.* 6: 931-957
- Fadare, O.O., Okoronkwo, A.E., Olasehinde, E.F. (2016). **Assessment of anti-corrosion potentials of extract of *Ficus asperifolia* - Miq (Moraceae) on mild steel in acidic medium.** *Africa J. Pure. App. Chem.* 10:8-22.
- Fouda, A.S., Al-Sharawy, A.A., El-Katori, E.E.** (2009). Pyrazolone derivatives as corrosion inhibitors for C-steel in hydrochloric acid solution. *Desalination*, 201(1-3):1-13.
- Hefang, W., Meidan, G., Yong G, Yongfang, Y., Rongbin, H.** (2016). A natural extract of tobacco rob as scale and corrosion inhibitor in artificial seawater. *Desalination.* 398: 198-207
- Khadom, A.A., Abd, A.A., Ahmed, N.A.** (2018). Xanthium strumarium leaves extracts as a friendly corrosion inhibitor of low carbon steel in hydrochloric acid: kinetics and mathematical studies. *South African Journal of Chemical Engineering*, 25, 13-21.
- Kliskic M., Radosevic J., Gudic S., Katalinic V.** (2000). Aqueous extract of *Rosmarinus officinalis* L. as inhibitor of Al-Mg alloy corrosion in chloride solution. *J. Appl. Electrochem.* 30(7): 823-830.
- Lebrini, M., Robert, F., Roos, C.** (2010). **Corrosion inhibition of C38 steel in 1 M hydrochloric acid medium by alkaloids extract from *Oxandra asbeckii* plant.** *Int. J. of Elect. Science*, 5 (11): 1698–1712.
- Li, X.H., Deng, S.D., Fu, H.** (2010). Inhibition by *Jasminum nudiflorum* Lindl. Leaves extract on the corrosion of cold rolled steel in hydrochloric acid solution. *J. Applied Electrochemical*, 40: 1641-1649 .
- Moorthy, S.K; Saravana, L.A.K.; Anandaram, S.** (2012). Anticorrosion potential of 4-Amino-3-methyl-1,2,4-triazole-5-thione Derivatives (SAMTT and DBAMTT) on mild steel in hydrochloric acid solution. *Industrial and Engineering Chemistry Research*, 51, 5408-5418.
- Obot, I.B., Obi-Egbedi, N.O., Umoren, S.A., Ebenso, E.E.** (2010). Synergistic and antagonistic effects of anions and *Ipomoea involucrata* as green corrosion inhibitor for aluminium dissolution in acidic medium. *Int J Electrochem Sci.* 5, 994-1007.
- Okafor, P.C, Ebenso, E.E.** (2007). Inhibitive action of *Carica papaya* extracts on the corrosion of mild steel in acidic media and their adsorption characteristics. *Pigment Res Technol.*, 36:134-140

- Olasehinde, E.F., Adesina, A.S., Fehintola, E.O., Badmus, B.M. and Aderibigbe, A.D.** (2012) Corrosion Inhibition Behaviour for Mild Steel by Extracts of *Musa sapientum* Peels in HCl Solution: Kinetics and Thermodynamics Study. *J. App. Chem.* 2:15-23.
- Olasehinde, E.F., Ogunjobi, J.K., Akinlosotu, O.M. and Omogbehin, S.A.** (2015). Investigation of the Inhibitive Properties of *Alchornea laxiflora* leaves on the Corrosion of Mild Steel in HCl: Thermodynamics and Kinetic Study *J. Am. Sci.* 11:1-8
- Olasehinde E.F., Olusegun S.J., Adesina A.S., Omogbehin S.A., Momoh-Yahayah,** (2013). Inhibitory Action of *Nicotina tabacum* Extracts on corrosion of Mild steel in HCl: Adsorption and Thermodynamic Study. *Nature and Science*, 11(1):83-90.
- Prabhu R. A., Venkatesha T. V., Shanbhag A. V., Praveen B. M., Kulkarni G. M. , Kalkhambkar R. G.** (2008). Quinol-2-thione compounds as corrosion inhibitors for mild steel in acid solution. *Mat. Chem. Phys.*, 108: 283-289.
- Patricia, E.A., Fiori-Bimbi, M.V., Neske, A., Brandan, A.S., Gervasi, A.C.** (2018). *Rollinia occidentalis* extract as green corrosion inhibitor for carbon steel in HCl solution. *J. Industrial and Engineering Chemistry*, 58, 92-99.
- Sivasankari, K., Janaky, R., Sekar, T.,** (2010). Evaluation of phytochemicals in select medicinal plants of the *Caesalpinia* species. *Ind. J. Sci and Tech.*, 3(12):1118-1121.
- Umoren, S.A.; Obot, I.B., Isreal, A.U., Asuquo, P.O., Solomon, U.M., Eduok, A.P.** (2014). Inhibiting of mild steel corrosion in acidic medium using coconut coir dust extracted from water and methanol as solvents. *Journal of industrial and Engineering Chemistry*, 20, 3612-3622
- Zhang X., Vu, T.-N., Volovitch P., Leygraf, G., Ogle, K., Odnevall, W. I.** (2012). The initial release of zinc and aluminum from non-treated Galvalume and the formation of corrosion products in chloride containing media. *Appl. Surf. Sci.* 258, 4351–4359.
- Zhang, Q.B., Hua, Y.X.** (2009). Corrosion inhibition of mild steel by alkylimidazolium ionic liquids in hydrochloric acid. *Elect. Acta.* 54:1881-1887.